Flight Optimization for Contrails and Emissions

A Large-Scale Trade-off Analysis Using Open Data and Models

Roosenbrand, E.J.; Sun, Junzi; Hoekstra, J.M.

Publication date
2024

Document Version
Final published version

Published in
Proceedings International Conference on Research in Air Transportation

Citation (APA)
Roosenbrand, E. J., Sun, J., & Hoekstra, J. M. (2024). Flight Optimization for Contrails and Emissions: A Large-Scale Trade-off Analysis Using Open Data and Models. In E. Neiderman, M. Bourgois, D. Lovell, & H. Fricke (Eds.), *Proceedings International Conference on Research in Air Transportation* Article ICRAT 2024-75

Flight Optimization for Contrails and Emissions

A Large-Scale Trade-off Analysis Using Open Data and Models

Esther Roosenbrand, Junzi Sun and Jacco Hoekstra
Faculty of Aerospace Engineering
Delft University of Technology
Delft, The Netherlands

***Abstract*—Emissions and contrails are key factors in aviation-induced climate change, often presenting conflicting objectives in flight trajectory optimization. Previous research typically lacks in optimizer efficiency or in addressing these trade-offs, with limited use of extensive meteorological and flight data. In this paper, a fully open non-linear optimal control flight optimization approach is designed for contrail avoidance and emission reduction, with high computational efficiency. This is achieved by leveraging the most recent trajectory optimizer, *OpenAP.TOP*, and atmospheric data handling tool, *fastmeteo*. We present a new compound grid-based objective function that considers both contrails and emissions and introduce four different metrics for evaluating the performance. A total of four months' worth of data, containing around half a million flights, are gathered from OpenSky for analyses. We show that high levels of contrail mitigation can be achieved, without significantly increasing flight time, distance, or emissions.**

***Keywords*—Sustainability, Contrails, OpenAP, Optimization, OpenSky, Aircraft Surveillance Data**

I. Introduction

Aviation is currently responsible for about 5% of net anthropogenic climate forcing [1]. This will cause increasingly escalating climate impacts as flight frequencies rise. Promising measures such as alternative fuels and aerodynamic aircraft design are under development. However, their large-scale commercial implementation is anticipated to take years or decades. In the urgency of addressing the climate crisis, sustainable aviation efforts should not only prioritize the advancement of these technologies but also focus on immediate implementations feasible for today's aircraft fleet.

A significant factor contributing to aviation's radiative forcing over shorter timescales is the formation of contrail cirrus, albeit with some uncertainties [2]. During the daytime, these contrails cause a parasol-like effect, where contrails scatter incoming solar radiation back to space, cooling the earth-atmospheric system below. During both night and day time, contrails trap terrestrial radiation, thereby restricting outgoing radiation and inducing a warming effect. There is scientific consensus that the net radiative effect of contrails is positive and thus has a warming effect on climate [1].

Unlike CO_2 emissions, which influence global warming over a span of 20–40 years, contrails have an immediate warming effect [3]. This emphasizes the need to minimize contrail formation as a way to limit aviation's climate impact immediately as well as into the future, similar to how fuel-optimization implements wind-optimization effectively in the flight planning.

Re-routing aircraft to avoid contrail formation generally leads to additional fuel burn [3], due to longer flight distances. Estimating this additional fuel burn requires a performance model to estimate the CO_2 emissions, and this is commonly performed with models like BADA or OpenAP [4]. In this paper, we adopt the open-source performance model OpenAP, and with integrated TOP [5] as a fully open four-dimensional flight trajectory optimizer.

For the first time, this paper formally presents the integration of contrail effects into OpenAP's optimization. Several contrail trajectory optimizers have been developed, ranging from the network-based contrail minimization approach [6] to optimizing individual trajectories [7].

The cost-functions used in previous work also differ, from ones based to aCCF's (algorithmic Climate Change Functions) [8] to time and cost optimization [9]. Our investigation has shown that because of sharp boundaries native to the aCCF data used, the trajectory optimizer has challenges with consistency and do not reliably provide realistic trajectories [8]. Additionally, we also find that the Kelvin / CO_2 kg metric used to fuel is hard coded into the aCCF algorithm and does not offer customization options in terms of trade-off or sensitivities studies.

In this paper, we adopt a fully 4D non-linear optimal control trajectory optimization approach, which considers the wind field and an objective function that considers both carbon emissions and contrail impacts. Our contrail-fuel-wind optimization is unique in its use of solely open-source data and code, in combination with the computational speed and customizability of the objectives.

For this study, we use 2023 ADS-B flight data from OpenSky, over both Europe and the United States, as a baseline to compare with the contrail-optimized trajectories. For each OpenSky flight that formed persistent contrails, several optimal trajectories are generated, which vary the level of emphasis placed on either contrail or emission prevention. Our analysis is focused on understanding the aggregated impacts and trade-offs among these different options.

This paper is structured as follows. Section II explains the background knowledge for the formation of persistent contrails. Section III gives an overview of the data we collected and used. Section IV provides the details on the methodologies for this study. Finally, Sections V, VI and VII include the results, discussions and conclusion from this study.

II. Contrail formation

Contrails are predominantly formed under the conditions with air temperatures lower than -40 °C (233 K) and high relative humidity [10]. For persistent contrail formation, two atmospheric conditions must be met:

1) Schmidt-Appleman Criterion (SAC), where the temperature must be below the critical temperature.
2) The ambient air is supersaturated with respect to ice ($RH_i > 100\%$), in an ice-supersaturated regions (ISSR).

The Schmidt-Appleman criterion (SAC) [10] is a thermodynamic model that takes into account ambient pressure, humidity, and the water-to-heat ratio in exhaust plumes. When an aircraft flies through atmospheric conditions that satisfy SAC, saturation with respect to liquid water occurs, and a contrail is formed.

The specific temperature threshold for contrail formation relies on the ambient relative humidity and the slope of the isobaric mixing line (G), which can be defined as follows:

$$G = \frac{EI_{H_2O}\ c_p\ p}{\varepsilon\ Q\ (1-\eta)} \tag{1}$$

where the constants for Eq. (1) can be found in Table I. In this paper, only cruise optimization is applied. A propulsion efficiency of η = 0.3 is assumed for modern aircraft–engine combinations [11].

In order to determine the threshold value T_{LC}, the temperature T_{LM} [10] must first be identified, which is given by:

$$T_{LM} = -46.46 + 9.43\ln(G - 0.053) + 0.72[\ln(G - 0.053)]^2 \tag{2}$$

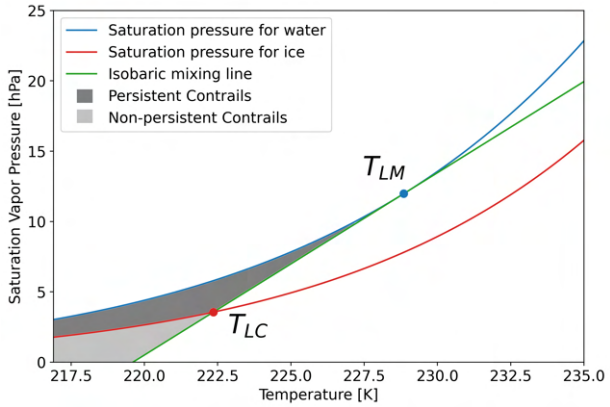

Figure 1. A visualization of the geometric approach to determining the critical formation temperature (T_{LC}), using the saturation pressure for water, the saturation pressure for ice and the isobaric mixing line with slope G at p_h = 230 hPa. Zones of contrails persistence are also indicated in the graph.

Subsequently, the mixing line is defined as the tangent line at the T_{LM} point with the saturation water vapour pressure curve (e^*). T_{LC} represents the intersection of the mixing line and the saturation water vapour pressure curve over ice. This geometric approach to identifying T_{LC} is visualized in Figure 1. The RH_i (%) can be calculated through the specific humidity (q in %):

$$RH_i = \frac{q\ p\ R_v}{R_d\ e_{ice}} \tag{3}$$

where e_{ice} (hPa) is the actual vapour pressure over ice [12]:

$$\log e_{ice} = 9.550426 - \frac{5723.265}{T} + 3.53068\ln(T) - 0.00728332T \tag{4}$$

where p is pressure, provided by the ERA5 data. R_v and R_d are gas constants for water vapour and dry air (see Table I).

For the study, we are only interested in minimizing the impact caused by persistent contrails.

TABLE I: Constants used for contrail formation

Symbol	Constant	Value	Unit
EI_{H_2O}	Emission index	1.2232	$-\ (kg_{H_2O}\ kg_{fuel}^{-1})$
c_p	Specific heat capacity air	1004	$J\ kg^{-1}\ K^{-1}$
ε	Ratio molar mass of water vapor and air	0.622	-
Q	Specific combustion heat	43×10^6	$J\ kg^{-1}$
η	Overall propulsion efficiency	0.3	-
R_v	Gas constant of water vapour	461.51	$J\ kg^{-1}\ K^{-1}$
R_d	Gas constant of dry air	287.05	$J\ kg^{-1}\ K^{-1}$

III. Data

In total, four full months of ADS-B flight data over the EU and USA are gathered and processed for this study, nearly half a million flights. This section explains the data sources and the steps taken before further processing.

A. ECMWF ERA5 dataset

The European Centre for Medium-Range Weather Forecasts (ECMWF) ERA5 dataset offers hourly atmospheric data on a high-resolution grid with a horizontal resolution of 0.25 degrees and 37 vertical layers. Conventionally, obtaining a large amount of ERA5 data from ECMWF and converting it into a format that can be used for aviation and optimization is a tedious process. To overcome this limitation for the research community, we released a new open-source tool *fastmeteo* [13], which allows researchers conveniently and rapidly incorporate any scale of ERA5 data in their research.

This study is one of the first that make use of *fastmeteo* on half million of flights, for both estimation of emissions and contrails, as well as make use of the meteorological information, such as wind, temperature, humidity in the optimization process.

B. OpenSky

The OpenSky Network has supported much of our previous research, and will be used again in this research. It has been collecting global air traffic surveillance data since 2013. The unfiltered and raw data from the OpenSky network is based on ADS-B, Mode S, TCAS and FLARM messages is open to use [14]. The variables used in this research include; time, latitude, longitude, callsign and the altitude.

OpenSky data for the months of January, April, July and October 2023, are downloaded. Flights that took off and landed within Europe or the United States are extracted for this study. The geographical regions of our flights are visualized in Figure 2. The red flights indicate persistent contrail formation at some point along the trajectory. The blue trajectories are non-contrail forming and are not considered for optimization.

The flights are then filtered and re-sampled to 30-second interval using the *traffic* library [15]. Almost half a million flights, which account for 20 GB of compressed data, are used for the study.

Table II shows the total number of persistent contrail forming flights (these are the ones considered in this study), as well as the percentage these flights are of the total. The total percent of persistent contrail forming flights is a weighted average based on the number of flights.

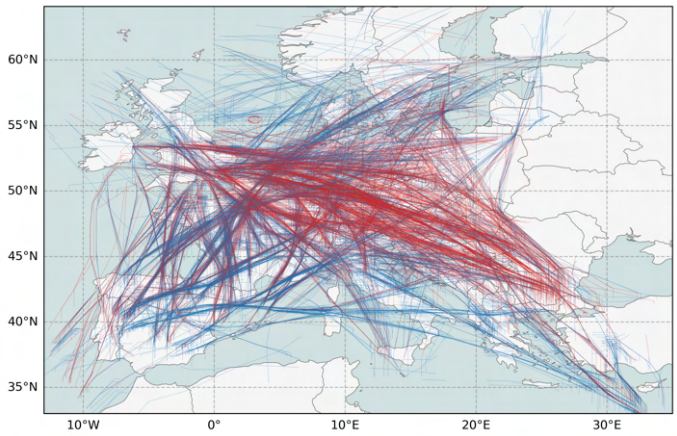

(a) The 2,877 flights trajectories considered for optimization in red on 6th of January 2023 in the European airspace.

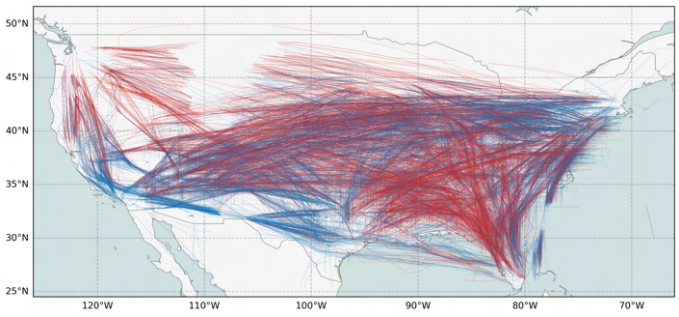

(b) The 2,519 flights trajectories considered for optimization in red on 5th of July 2023 in the airspace over the United States of America.

Figure 2. All cruise section of flights for a single day above the European and United States airspace. The red flights indicate persistent contrail formation at some point along their trajectory. The blue trajectories are non-contrail forming.

TABLE II: Flights Considered

	January	April	July	October	Total
# contrail flights	178,534	114,160	72,688	101,589	466,971
[%]	9.1	4.8	4.2	6.7	6.8

C. Processing of Data

Each individual trajectory is converted into a traffic [15] type and assigned a unique flight identification number. For each flight trajectory, the ADS-B data points where persistent contrails are created are determined using *fastmeteo*, according to the two atmospheric conditions described in Section II.

The *fastmeteo* module [13] allows for quick weather-data interpolation based on ECMWF's ERA5 data, using a client-server architecture via an API. Weather data from the nearest hour to the flight's takeoff time is used.

Once all the contrail-forming flights are gathered, the trajectories are resampled at every 15 seconds to fill data gaps. Subsequently, the flight is clipped to the trajectory between top of climb and top of descent.

Using the *.phases* function from *traffic*, the flight phases are determined for each ADS-B measurement point. This phase library is based on the fuzzy logic flight phase identification algorithm from OpenAP [4]. Trajectory optimization is performed solely during the cruise phase of the flight, since optimization during ascent and descent is not possible.

IV. Methodology

In this section, we focus on explaining the optimization, the creation of the contrail-based cost function, and the research approach applied to compare OpenSky ADS-B trajectories with the resulting optimized trajectories.

A. The trajectory optimizer

The trajectories are optimized using the *OpenAP.TOP* optimizer. This optimizer models the trajectory optimization as a non-linear optimal control problem, where speed, vertical rate, and heading are considered as the control variable. Based on a direct collocation method, the optimal discretized flight trajectory is computed to minimize a desired objective function, such as fuel, cost index, or any other customized objectives.

In our previous study [5], the internal of the *OpenAP.TOP* optimizer is discussed in detail. It is built on top of the OpenAP model, and a common optimization framework called *Casadi*, which uses the *IPOPT* as the nonlinear programming solver.

The optimizer is made open-source[1] due to the fact that all components, including the underlying aircraft performance model, the optimization framework, and the nonlinear programming solver, are all openly shared.

In this study, our focus is on designing a new three-dimensional discretized objective grid, that can be used to consider the trade-off between contrails and emissions at all locations, at any given scale. The optimization of a trajectory can be generally completed in the tens of seconds on a single core with a modern computer. And the optimization of multiple flights can be computed in parallel with multiple cores.

B. Using convolutions to smooth objective boundaries

As described in Section II two conditions must be met for persistent contrail formation to occur, namely the temperature to be below a critical temperature, and the RH_{ice} exceeding 100%.

A binary mask is created where grid points that meet these two conditions are set to one, and the rest are set equal to zero. The contrail-optimizer will avoid grid values of one, as these are persistent contrail forming regions.

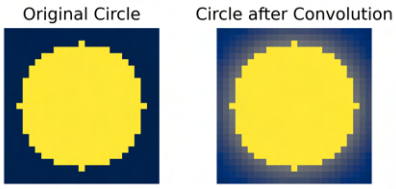

Figure 3. Example of the convolution applied to the binary contrail forming grid, where the binary ones are retained, and only convolution is applied to the surrounding zeros.

To ensure a smoother cost grid function and thus more realistic trajectories, a kernel of 5 by 5 pixels (1.25 x 1.25 degrees) is applied to each altitude level using two-dimensional convolution. The convolution is performed so that the binary values equal to one remain intact, while the surrounding pixels are increased in value, using the SciPy *convolve2d* function [16].

This convolved contrail array (see Section III-A) subsequently was scaled to be a similar weight to the fuel parameter, in order to achieve an effective cost function.

[1]Accessible at https://github.com/junzis/openap-top

C. Optimal trajectory with new contrail-emission costs

As previously mentioned, the OpenAP.TOP optimizer allows the use of grid-based cost function, which is a unique feature of the optimizer. Such capability allows grid-like and discontinuous objectives to be rapidly adopted in the flight optimization.

Such a feature is essential for generation of optimal flights considering contrails, as the meteorological condition for contrail formation is highly irregular and temporally dynamic. From each flight's top of climb to the top of descent location, the atmospheric conditions at the nearest hour to the flight's takeoff time are used to generate the optimal trajectories. An example of the grid cost based on persistent contrail formation condition is illustrated in Figure 4.

The unique compound cost function presented in this paper offers minimization between both fuel usage and contrail formation, with a user defined coefficient between the two. The cost function was constructed through a process of trial-and-error, until a cost function was obtained exhibiting the behaviour required.

Because the cost function should properly balance contrail formation against additional fuel burn, the following structure was selected:

$$\text{Cost Function} = C_{oi} \cdot \text{Contrail} + (1 - C_{oi}) \cdot \text{Fuel} \quad (5)$$

where the coefficient (C_{oi}) indicates the user defined coefficient, which is also referred to as *Coefficient of Impact* (CoI) in the rest of this paper.

Additionally, besides this contrail-optimized trajectory, a solely fuel-optimized route is also calculated using OpenAP.TOP's default minimal fuel objective. In all optimizations, wind conditions, along other meteorological parameters, are obtained using *fastmeteo*. The computation speed of incorporating meteorological conditions is at sub-second.

D. Metrics used for comparison and evaluation

In this study, we design four metrics to compare the OpenSky trajectory, the fuel-optimized trajectory, and the contrail-optimized trajectories. These metrics are:

1) Δt: represent the change in flight time,
2) Δd: represent the difference in flight distance,
3) $\Delta t_{\text{contrail}}$: reduction in time of persistent contrails
4) ΔCO_2: changes in CO_2 emissions.

After determining whether persistent contrails formed in the flight's local atmospheric conditions, the total time of persistent contrail formation during the flight is calculated. Subsequently, this time was calculated as a percentage of the OpenSky trajectory flight time, which serves as a baseline.

The change in CO_2 emissions are calculated using OpenAP [4] with the flight trajectory data with the mass assumption of 90% of maximum takeoff weight at the start of the trajectory.

All previously defined four metrics (flight time, flight distance, contrail time, and CO_2) were calculated in absolute terms, as well as a percentage of change with the OpenSky ADS-B trajectory as a baseline compared with both the contrail-minimized and fuel-optimized trajectories.

V. Analyses and Results

In this section, the contrail-minimizing optimization is evaluated against the baseline of the ADS-B OpenSky trajectories. This evaluation is done through the comparison metrics presented in the previous section, namely, the additional flight time and distance flown, as well as the change in time flown in persistent contrail forming areas (or *contrail time*), and additional CO_2 emissions.

To best illustrate the results and the meaning of the aforementioned metrics, two random flights are highlighted in the following sections, after which histograms containing all 466,971 flights are shown.

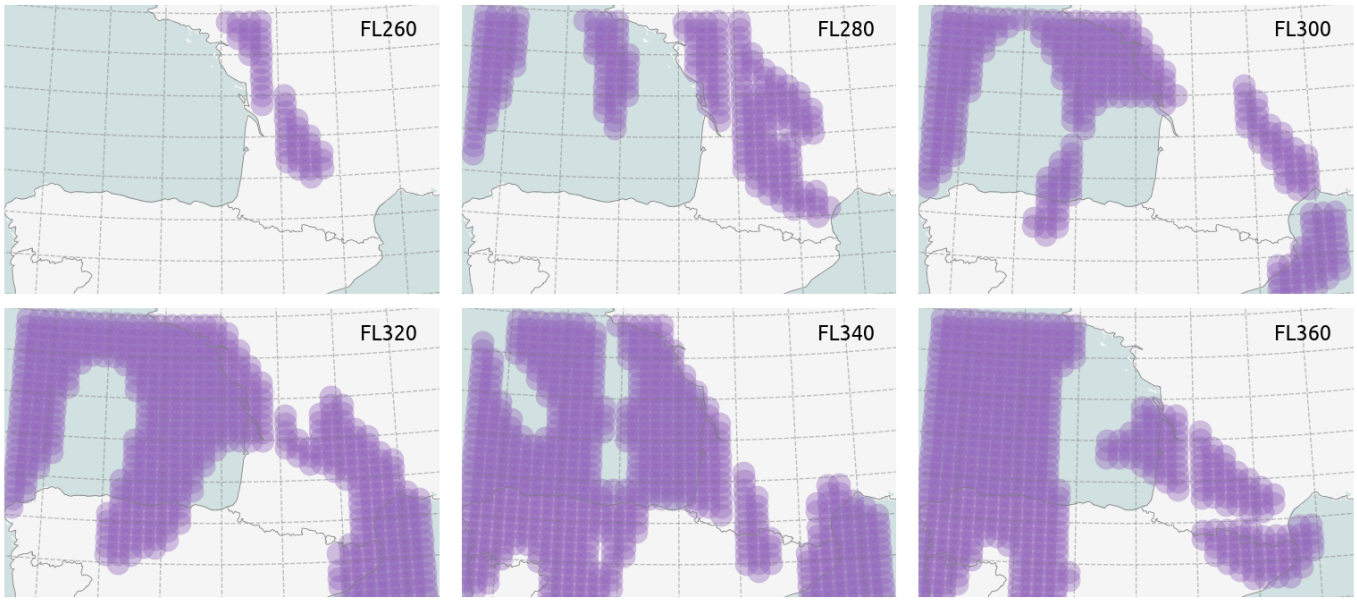

Figure 4. Illustration of the 3D cost grid based on the conditions for persistent contrails. Only flight levels between FL260 and FL360 are shown. The actual grid spans between FL100 and FL400.

A. Examples of optimal trajectories

In Figure 5, optimization of flight ABR255 from Paris to Hanover on the 19th of July 2023 is shown, with the cruise section of the OpenSky trajectory in blue. Darkening of the colours represent an increase of altitude.

The red underlying circles indicate the measurements are located in persistent contrail forming conditions. The background is the convoluted persistent contrail forming grid, ranging from transparent (zero indicating no contrail formation) to dark grey (one indicating persistent contrail formation).

Not all red circle contrail locations appear to correlate with the contrail grid values, because only one altitude of the contrail forming grid can be shown. The altitude, shown in the grid, is represented as a horizontal line in the altitude plot insert.

The yellow trajectory shows the fuel-optimized trajectory, which neatly follows the great circle, as winning time through wind optimization is not possible, because of a weak local wind (average of 14.3 m/s). Again, here, red circles indicate contrail forming conditions.

Three green contrail-optimal routes are shown with varying the CoI from 0.8 (in bold) to 0.4 to 0.2, with the latter being closest to the great circle. In Table III the four comparison metrics are shown for each of the CoI's. The absolute values are shown, as well as the relative percent change with the OpenSky trajectory.

Table III and Fig. 5 show that a CoI of 0.8 does not fly through *any* persistent contrail forming conditions (100% reduction of contrail flight time, from 8.5 minutes). However, this high CoI adds the most additional flight time, the most additional distance as well as the largest CO_2 emissions increase.

In Figure 5 the plot insert shows the altitude changes throughout the flight, as well as the locations of persistent contrail forming conditions. As expected, the fuel-optimized route has a higher altitude than the original OpenSky trajectory.

The contrail-optimized routes not only show a clear departure in the horizontal plane (adding a maximum distance of 6% or 14 kilometres), but also in the vertical, with a strong altitude increase in order to avoid persistent contrail forming conditions. While still flying higher than the fuel-optimized route, because of the sharp altitude increase the contrail-optimized route increases CO_2 emissions by 4%.

TABLE III: Comparison Metrics for Varying Coefficients, ABR255

CoI	Δt	Δd	$\Delta t_{\text{contrail}}$	ΔCO_2
0.8	02:32 (+13%)	08:31 (-100%)	14.8 (+6%)	+4%
0.4	02:07 (+11%)	07:30 (-88%)	6.7 (+3%)	+3%
0.2	00:57 (+5%)	05:58 (-70%)	1.2 (+0.5%)	+1%

A second example of the optimization is visualized in Figure 6, flight AF1195 on the 7th of April 2023. As indicated by the red circles, along a large section of the OpenSky and fuel-optimized trajectories, persistent contrail forming conditions are encountered.

As visualized in Figure 6, the more favourable local wind field at a lower altitude cause the fuel-optimal route to fly lower than the OpenSky trajectory. This results in a flight time reduction of 6% compared to the OpenSky trajectory.

However, the fuel-optimal route (in yellow) increases the time flown in persistent contrail forming areas, by 37% compared to the OpenSky trajectory. Table IV shows that the contrail-optimized routes still offer the benefit of a flight time reduction, while *additionally* effectively minimizing contrail formation.

TABLE IV: Comparison Metrics for Varying Coefficients, AF1195

CoI	Δt	Δd	$\Delta t_{\text{contrail}}$	ΔCO_2
0.8	04:42 (-5%)	12:31 (-79%)	20.8 (+1.5%)	+2
0.4	03:32 (-4%)	05:10 (-31%)	15.2 (+1.1%)	0
0.2	0:57 (-1%)	02:58 (-19%)	-8 (+0.6%)	-1

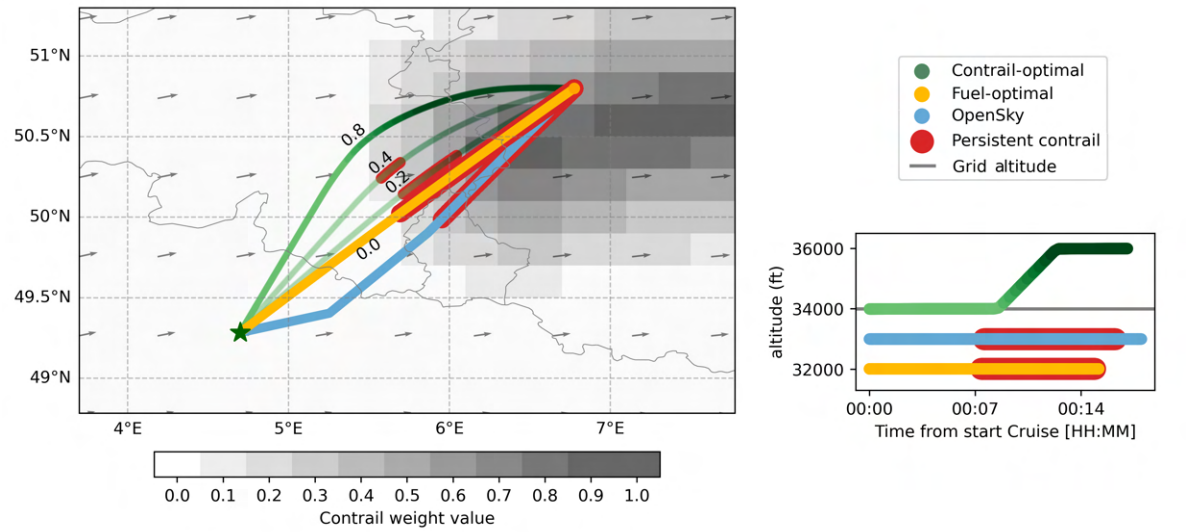

Figure 5. Flight ABR255 Paris to Hanover on 19 July 2023. The optimization and the OpenSky trajectory are shown. Several green contrail-optimal routes are indicated with varying CoI's (as indicated by number). The background is the convoluted persistent contrail forming grid, ranging from transparent (zero values indicating no contrail formation) to dark grey (one values indicating persistent contrail formation). The figure insert shows the altitude change in time for the three trajectories. The altitude shown in the left grid, is represented as a horizontal line in the altitude plot insert.

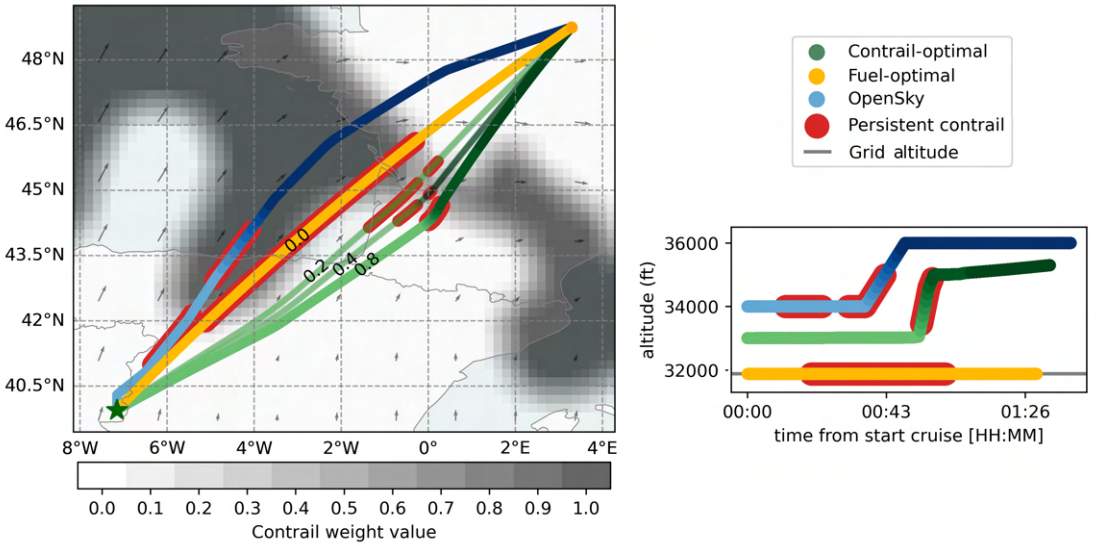

Figure 6. Flight AF1195 Lisbon to Paris on 7 April 2023. The optimization and the OpenSky trajectory are shown. Several green contrail-optimal routes are indicated with varying CoI's (as indicated by number). The background is the convoluted persistent contrail forming grid, ranging from transparent (zero values indicating no contrail formation) to dark grey (one values indicating persistent contrail formation). The figure insert shows the altitude change in time for the three trajectories. The altitude shown in the left grid, is represented as a horizontal line in the altitude plot insert.

B. All flights

In this section, we provide the aggregated statistics of all 466,971 flights, and the histograms of all these flights are shown for each of the four metrics discussed earlier.

1) Changes in flight time: First, Figure 7 shows the histograms for the change in total flight time using a CoI of 0.8, so more weight placed on contrail mitigation than minimizing fuel burn.

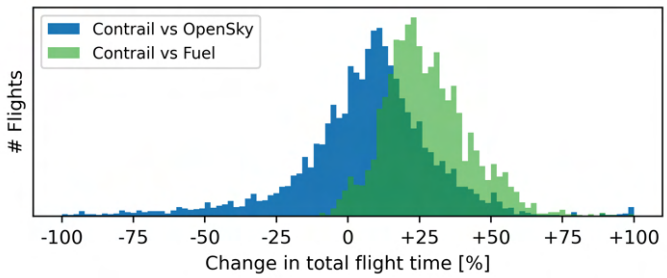

Figure 7. Histogram of the change in flight time for Contrail optimized vs OpenSky (blue) and Contrail vs Fuel Optimized (green) at CoI value 0.8.

The total flight time of the OpenSky and the contrail optimized trajectory are calculated. The histograms show the difference between the two times, as a percent change of the OpenSky trajectory time, in blue. In green, the same procedure is applied to the fuel and contrail optimized trajectory times.

The histograms indicate that on average, the contrail optimized trajectories have a longer total flight time (mean of 4.6% and a median of 8.3%) than the flown OpenSky trajectories.

As the fuel optimized route is in a sense also time-optimized, it follows that the change between the fuel and contrail optimization is larger than for the OpenSky trajectory, which is visible in Figure 7.b (mean of 27.6% and a median of 25.6%).

To investigate the impact of the Coefficient of Impact (CoI), Figure 8 shows several Ridgeline plots of the change in time spent in persistent contrail regions for varying CoI.

To limit computation time, the histograms were generated for a single month (April) only.

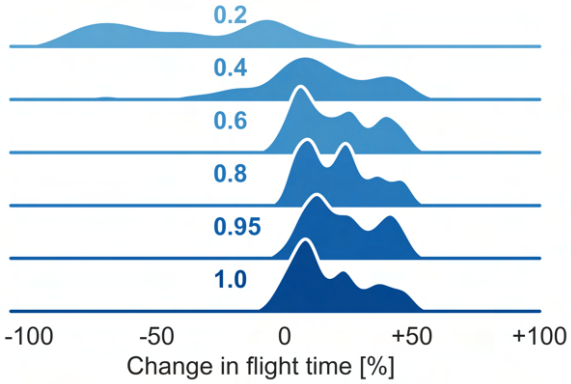

Figure 8. Ridgeplot histograms of change in flight time with varying Coefficient of Impact (CoI) with respect to the flown OpenSky trajectories.

2) Changes in persistent contrail time: The second set of histograms in Figure 9 show the change in time flown in persistent contrail forming conditions (or *contrail time*). A high CoI, at the ratio of 1, prioritizes avoiding flying in persistent contrails conditions. In this extreme situation, 42% of original contrail-forming flights could have produced no persistent contrails at all any more (i.e., -100% reduction).

Figure 9 also shows that even at low CoI, the majority of flights could have reduced their persistent contrails by 80%. By lowering the CoI, the tail of the histogram grows, and contrail mitigation becomes less definitive.

3) Changes in flight distance: Figure 10 shows a histogram indicating the change in the flown distance. The distribution of the contrail-optimized vs OpenSky trajectories exhibit a normal distribution centred around zero.

The ridgeplots for varying CoI are shown in Figure 11. As fuel optimization is similar to optimizing for time and distance, it follows that without exception, the contrail-optimized routes are longer (mean of 6.1% and a median of 5.0%).

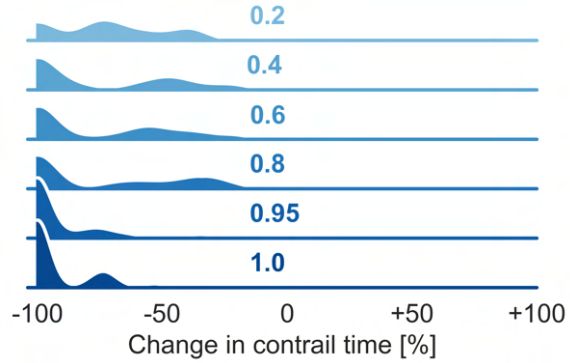

Figure 9. Ridgeplot histograms of change in contrail time with varying CoI

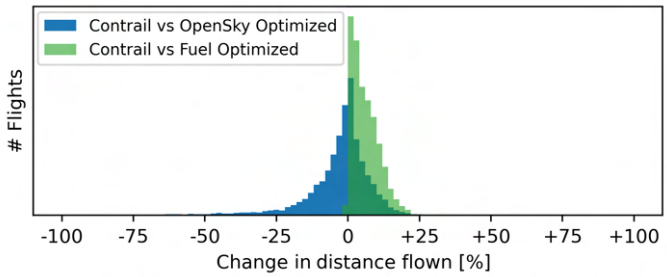

Figure 10. Histogram of the change in flown distance, vertical axis is the same scale in both graphs at CoI value 0.8.

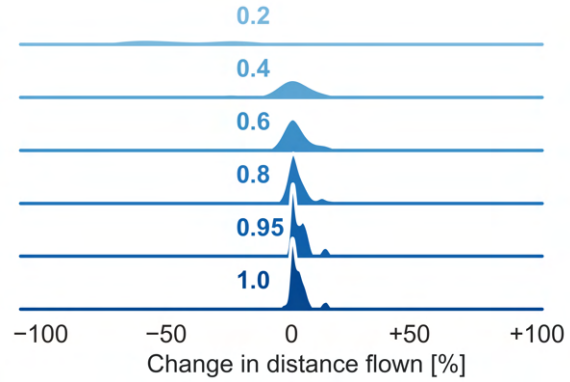

Figure 11. Ridgeplot histograms of change in distance flown with varying CoI.

4) Changes in emissions: In Figure 12 a similar story to Figure 7 is shown, where generally, CO_2 emissions are increased more in the contrail-optimized trajectories than the fuel-optimized trajectory (mean of 29.4% and a median of 28.8%). The same is also true for the OpenSky baseline (mean of 10.8% and a median of 12.4%). The ridgeplots for varying CoI's are shown in Figure 13.

VI. Discussions

A. Influence of the CoI

In this study, we have shown that the coefficient in the customizable objective function has significant influence on the optimality of the trajectory concerning flight time and emissions.

In Figure 9, the two example flights in Figures 5 and 6 and Table III shows that a high CoI is extremely effective at reducing time flown in persistent contrail regions. However,

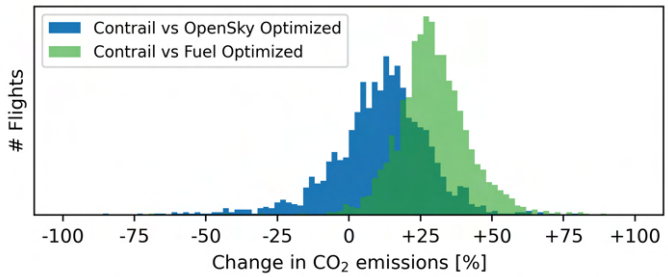

Figure 12. Histogram of the change in CO_2 emissions, vertical axis is the same scale in both graphs, at CoI value 0.8.

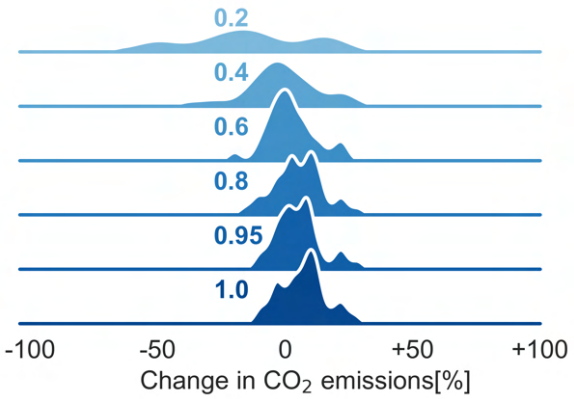

Figure 13. Ridgeplot histograms of change in CO_2 emissions with varying CoI

while a lower CoI still remains effective against contrail time, the CO_2 emissions and distance penalties are considerably less.

B. Cooling effect of the contrails

As described in the Introduction, contrails can have both warming and cooling effects on the climate, although the net radiative effect of contrails is positive and so warming.

Currently, the cost function presented in this paper is constructed as a Coefficient of Impact (CoI) between avoiding persistent contrail forming regions and fuel. This means that forming potentially cooling contrails is also avoided. In future work, based on meteorological and geographical data a prediction can be made whether the persistent contrail formed will be warming or cooling can be made. Besides this incorporation, instead of a CoI between contrails and fuel, a radiative forcing based ratio could be used.

C. Seasonal effects

Although air traffic reaches its peak during the summer months in the Northern Hemisphere, [3] and [17] note a higher incidence of persistent contrails in winter. Table II confirms this pattern; despite the lowest total number of flights, as expected, the percentage of flights producing contrails is highest during the winter months. This implies that, potentially, re-routing in these contrail prevalent months can be done more easily due to lower traffic volumes.

D. Safety of diverted flight trajectories

In this paper, each trajectory is optimized individually and the complete air network is not taken into account.

This implies that it is possible for two flights post-optimization to no longer be horizontally or vertically separated. However, safety impacts are minimal [17], with only a slight increase in the number of intrusions or conflicts when changing altitudes for contrail prevention.

E. Uncertainty ERA-5 weather data

The presence of persistent contrails is determined using ECMWF's ERA5 dataset through the temperature and specific humidity parameters. The temperature condition mentioned in II can be predicted reliably [18].

However, the specific humidity parameter has some problems with reliability, especially in the upper troposphere. The level of relative humidity over ice is often underestimated [19]. This leads to lower estimates of the instantaneous radiative forcing [18].

F. Improvements Schmidt-Appleman Criterion

In this paper, a propulsion efficiency of $\eta = 0.3$ is assumed for modern aircraft–engine combinations. However, in Eq. (1) η is defined as the fraction between resulting energy (thrust and true air speed) and required energy (specific combustion heat Q and fuel flow) [10]. In future work, this parameter should be dynamic and not assumed constant.

VII. Conclusion

This paper presents a fully open-source flight optimizer for contrail-avoidance based upon the *OpenAP* model and atmospheric data from *fastmeteo*. By introducing a new grid-based objective function that considers impacts of both contrails and carbon emissions, optimal trajectories can be generated with different degrees of trade-off between contrail avoidance and excess emissions.

To analyse our approach, four months of OpenSky flight data from 2023 were gathered and evaluated based on four metrics; flight time and distance, time spent in persistent contrail forming regions as well as the CO_2 emissions.

From this analysis of these four metrics of 466,971 flights, we show that while tuning the CoI to prioritize contrail mitigation is very effective (85% reduction in contrail time), it penalizes flight time (+5%) and distance (+6%) heavily.

Furthermore, an important discovery based on our analysis, we can conclude that a large amount of contrails can be mitigated even with a lower CoI, without much penalty on additional distance flown, flight time, or CO_2 emissions.

For future studies, we will further explore a climate-optimized routing model, which deals with energy forcing by modeling the warming or cooling effects based on varying atmospheric conditions. The methods and analysis in this paper have paved a path for the generation of a climate-optimal routing model using solely the open data and open models.

Reproducibility Statement

The source code for the optimization study in this paper is available at: https://github.com/junzis/openap-top.

References

[1] D. Lee, "The contribution of global aviation to anthropogenic climate forcing for 2000 to 2018.," *Atmospheric Environment*, vol. 244, 2021.

[2] V. Grewe, K. Dahlmann, J. Flink, C. Frömming, R. Ghosh, K. Gierens, R. Heller, J. Hendricks, P. Jöckel, S. Kaufmann, *et al.*, "Mitigating the climate impact from aviation: Achievements and results of the dlr wecare project," *Aerospace*, vol. 4, no. 3, p. 34, 2017.

[3] D. Avila, L. Sherry, and T. Thompson, "Reducing global warming by airline contrail avoidance: A case study of annual benefits for the contiguous united states.," *Transportation Research Interdisciplinary Perspectives*, vol. 2, 2019.

[4] J. Sun, J. M. Hoekstra, and J. Ellerbroek, "Openap: An open-source aircraft performance model for air transportation studies and simulations," *Aerospace*, vol. 7, no. 8, p. 104, 2020.

[5] J. Sun, "Openap.top: Open flight trajectory optimization for air transport and sustainability research," *Aerospace*, vol. 9, no. 7, p. 383, 2022.

[6] C. Demouge, M. Mongeau, N. Couellan, and D. Delahaye, "A time-dependent subgraph-capacity model for multiple shortest paths and application to co2/contrail-safe aircraft trajectories," 2023.

[7] A. Simorgh, M. Soler, D. González-Arribas, F. Linke, B. Lührs, M. M. Meuser, S. Dietmüller, S. Matthes, H. Yamashita, F. Yin, *et al.*, "Robust 4d climate-optimal flight planning in structured airspace using parallelized simulation on gpus: Roost v1. 0," *Geoscientific model development*, vol. 16, no. 13, pp. 3723–3748, 2023.

[8] F. Yin, V. Grewe, F. Castino, P. Rao, S. Matthes, K. Dahlmann, S. Dietmüller, C. Frömming, H. Yamashita, P. Peter, *et al.*, "Predicting the climate impact of aviation for en-route emissions: the algorithmic climate change function submodel accf 1.0 of emac 2.53," *Geoscientific Model Development*, vol. 16, no. 11, pp. 3313–3334, 2023.

[9] J. Rosenow, H. Fricke, and L. Sherry, "Time of the day-dependent impact of contrail avoidance strategies on airline delay costs," in *Proceedings of the Fifteenth USA/Europe Air Traffic Management Research and Development Seminar (ATM2023), Savannah, GA, USA*, pp. 5–9, 2023.

[10] U. Schumann, "Formation, properties and climatic effects of contrails," *Comptes Rendus Physique*, vol. 6, no. 4-5, pp. 549–565, 2005.

[11] A. Rap, P. Forster, A. Jones, O. Boucher, J. Haywood, N. Bellouin, and R. De Leon, "Parameterization of contrails in the uk met office climate model," *Journal of Geophysical Research: Atmospheres*, vol. 115, no. D10, 2010.

[12] D. M. Murphy and T. Koop, "Review of the vapour pressures of ice and supercooled water for atmospheric applications," *Quarterly Journal of the Royal Meteorological Society: A journal of the atmospheric sciences, applied meteorology and physical oceanography*, vol. 131, no. 608, pp. 1539–1565, 2005.

[13] J. Sun and E. Roosenbrand, "Fast contrail estimation with opensky data," *Journal of Open Aviation Science*, vol. 1, no. 2, 2023.

[14] M. Strohmeier, X. Olive, J. Lübbe, M. Schäfer, and V. Lenders, "Crowdsourced air traffic data from the opensky network," 2021.

[15] X. Olive, "traffic, a toolbox for processing and analysing air traffic data," *Journal of Open Source Software*, vol. 4, p. 1518, 2019.

[16] P. Virtanen, R. Gommers, T. E. Oliphant, M. Haberland, T. Reddy, D. Cournapeau, E. Burovski, P. Peterson, W. Weckesser, J. Bright, S. J. van der Walt, M. Brett, J. Wilson, K. J. Millman, N. Mayorov, A. R. J. Nelson, E. Jones, R. Kern, E. Larson, C. J. Carey, İ. Polat, Y. Feng, E. W. Moore, J. VanderPlas, D. Laxalde, J. Perktold, R. Cimrman, I. Henriksen, E. A. Quintero, C. R. Harris, A. M. Archibald, A. H. Ribeiro, F. Pedregosa, P. van Mulbregt, and SciPy 1.0 Contributors, "SciPy 1.0: Fundamental Algorithms for Scientific Computing in Python," *Nature Methods*, vol. 17, pp. 261–272, 2020.

[17] E. Roosenbrand, J. Sun, and J. Hoekstra, "Contrail minimization through altitude diversions: A feasibility study leveraging global data," *Transportation Research Interdisciplinary Perspectives*, vol. 22, p. 100953, 2023.

[18] K. Gierens, S. Matthes, and S. Rohs, "How well can persistent contrails be predicted?," *Aerospace*, vol. 7, no. 12, 2020.

[19] S. M. Hofer, K. M. Gierens, and S. Rohs, "How well can persistent contrails be predicted? – an update," *EGUsphere*, vol. 2024, pp. 1–24, 2024.